

# PLANAR BILAYER MEMBRANES MADE FROM PHOSPHOLIPID MONOLAYERS FORM BY A THINNING PROCESS

WALTER D. NILES, RICHARD A. LEVIS, AND FREDRIC S. COHEN  
*Rush Medical College, Department of Physiology, Chicago, Illinois 60612*

**ABSTRACT** We investigated the manner in which planar phospholipid membranes form when monolayers are sequentially raised. Simultaneous electrical and optical recordings showed that initially a thick film forms, and the capacitance of the film increases with the same time course as the observed thinning. The diameter of fully thinned membranes varies from membrane to membrane and a torus is readily observed. The frequency-dependent admittance of the membrane was measured using a wide-bandwidth voltage clamp whose frequency response is essentially independent of capacitative load. The membrane capacitance dominates the total admittance and the membrane dielectric is not lossy. The specific capacitance of membranes of several mixtures was measured. A schematic diagram of the formation of these membranes is presented.

## INTRODUCTION

There are two basic methods for forming phospholipid bilayer membranes. In the first, lipid is dissolved in a nonvolatile hydrocarbon solvent. A small quantity of this membrane-forming solution is applied to a hole in a sheet, typically made of Teflon, separating two aqueous compartments. The hydrocarbon drains into a Gibbs-Plateau border (known as a torus), which surrounds the thin film that forms (Mueller et al., 1963). This thin film, referred to as a black lipid membrane (BLM), consists of a phospholipid bilayer with a considerable amount of dissolved solvent (Hanai et al., 1965; White, 1972). In the second method, bilayers are formed from monolayers as originally described by Takagi et al. (1965) and modified by Montal and Mueller (1972). Monolayers spread at two air-water interfaces are sequentially raised over a hole that has been pretreated with hydrocarbons such as Vaseline or squalene (Montal, 1974; Reyes and Latorre, 1979), and a phospholipid bilayer forms where the monolayers meet. These latter membranes, which we refer to as MM films, are relatively solvent-free. They are commonly described as forming via the direct apposition of the two monolayers (Montal, 1974; White et al., 1976).

Here we report simultaneous optical and electrical studies showing that contrary to the common view, sequential raising of the monolayers results initially in the formation of a thick hydrocarbon-phospholipid mixture within the hole. Only when the hydrocarbon drains does a bilayer form. When the membrane has fully thinned, a visually apparent torus surrounds the bilayer. By measuring the area of thinned MM membranes and using a specially constructed wide-bandwidth voltage clamp, we measured the specific capacitance of the bilayer.

## METHODS AND MATERIALS

Planar membranes were formed by sequentially raising monolayers past a 50–300- $\mu\text{m}$  diam hole in a partition separating the two aqueous compartments. Teflon partitions, varying in thickness from 1 to 5 ml, (Dilectrix, Lockport, NY), were used when the hole was pretreated with squalene. A Saran wrap partition (Dow Chemical, Indianapolis, IN) was used when the hole was precoated with petroleum jelly (Vaseline; Cheesebrough-Ponds, Greenwich, CT). The chamber, milled from Teflon, had glass coverslips (0.17-mm thick) as front and rear walls, which provided an unobstructed light path. Ag/AgCl electrodes were placed in each compartment through holes bored in the Teflon chamber and connected to the headstage of the voltage clamp.

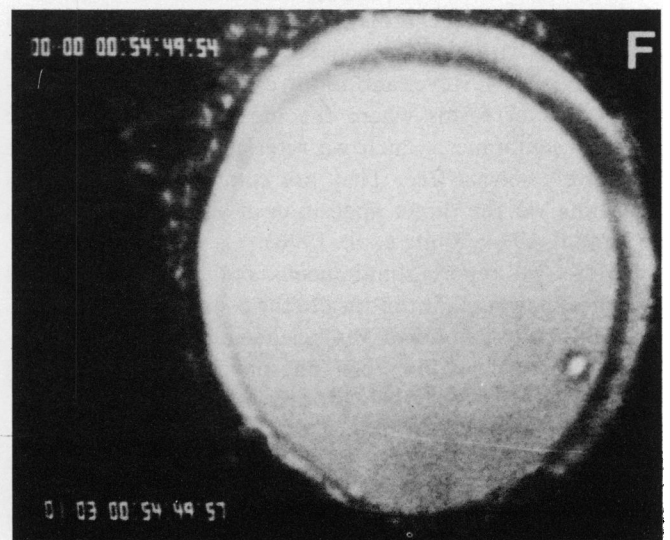
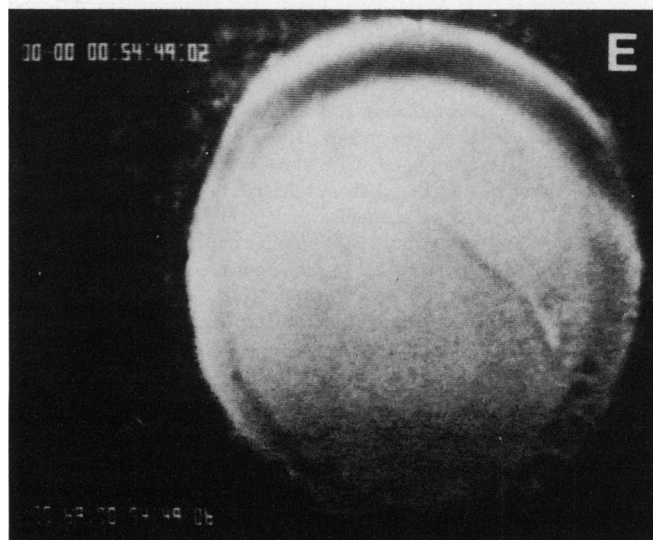
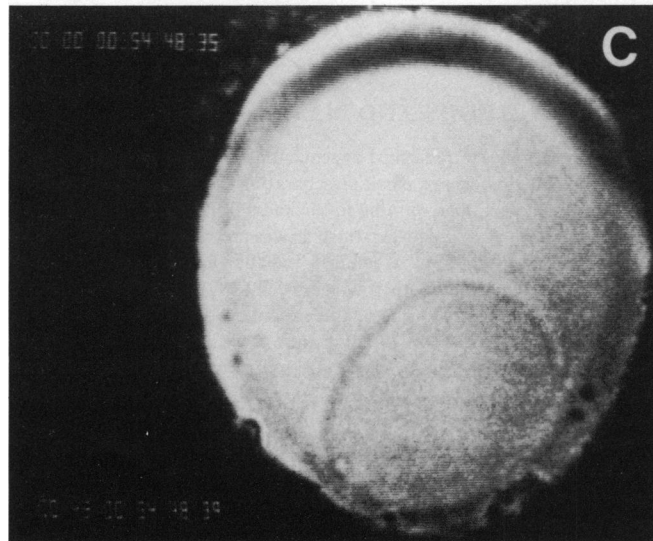
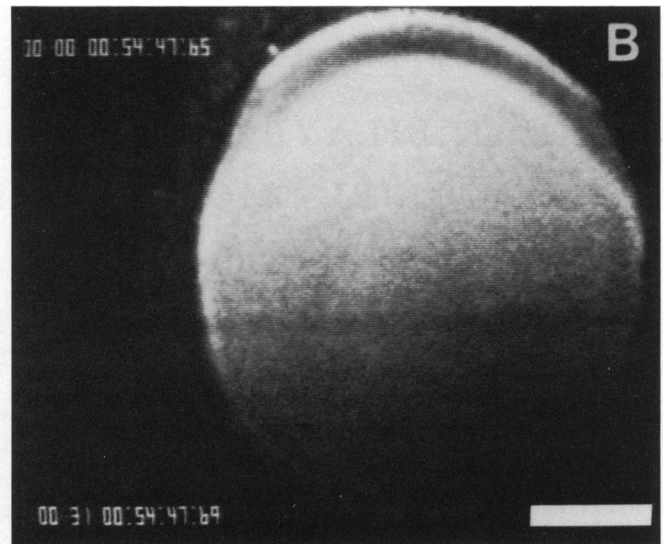
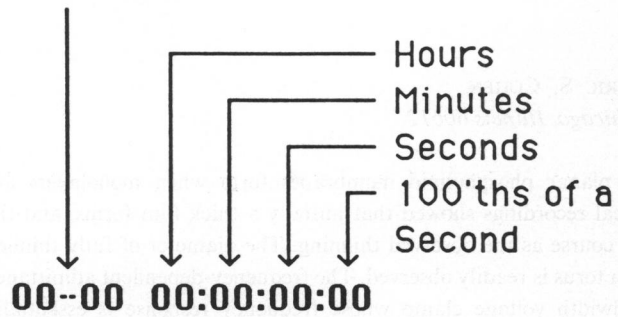
Membranes were formed either from asolectin (Type IVS; Sigma Chemical Co.) washed by the procedure of Kagawa and Racker (1971), bacterial phosphatidylethanolamine (BPE), PE prepared by transphosphatidylation of egg lecithin in the presence of ethanolamine (TPE), or diphytanoyl phosphatidylcholine (DPC). The latter three phospholipids were purchased from Avanti Polar Lipids, Inc. (Birmingham, AL) and used as received. Monolayers were spread by applying 10 and 5  $\mu\text{l}$  of a 1% lipid/hexane (Burdick & Jackson Laboratories Inc., Muskegan, MI) solution (wt/vol) to the larger (1.5 ml) and smaller compartments (0.7 ml), respectively. Solvents were allowed to evaporate for up to 30 min before the monolayers were raised. Holes in Teflon partitions were pretreated with (typically) 4  $\mu\text{l}$  of 1% squalene (Sigma Chemical Co.) in pentane (Burdick & Jackson Laboratories Inc.) (vol/vol). The squalene was passed over an activated alumina column. Holes in Saran wrap were treated with the supernatant of 15% Vaseline in petroleum ether (Baker Co., Sanford, ME) (wt/vol). The membranes were bathed with symmetrical solutions of 400 mM KCl, 10 mM Hepes, 3 mM  $\text{MgCl}_2$ , 1mM EDTA, pH 7.5. Milli-Q water (Millipore Corp., Bedford, MA) was used for all solutions (18 M  $\Omega\text{-cm}$ ).

To observe the formation of membranes, we used a setup previously described in detail (Niles and Cohen, 1987). In brief, a microscope (Laborlux 11; E. Leitz, Inc., Rockleigh, NJ) without a stage was laid on its back brace and bolted to an air table. The chamber, placed where the stage would normally go, was mounted in a Lucite holder attached to a micromanipulator. The membrane was brought into focus with the micromanipulator and was illuminated by transmitted light from a brightfield source. This light was passed through a Nikon MPlan

00--00 00:00:00:00

**A**

Capacitance



20X/NA 0.4 ELWD objective with a working distance of 11 mm, and then through a 15× eyepiece placed in tandem with a 0.3× projection lens. The resulting image was focused onto the photocathode of a SIT video camera (SIT 66; Dage-MTI Inc., Michigan City, IN). The video signal was displayed on a video monitor (V20; Elecrohome Ltd., Canada). The position of the 15× eyepiece was varied for each size hole so that the image of each hole filled the screen of the monitor. The total magnification of the system when a 150-μm hole was used was 1,000. The video signal was recorded on 3/4-in. U-matic format tape with a Sony VO5800H videotape recorder.

The voltage clamp headstage amplifier consisted of a discrete junction field-effect transistor (JFET) (U430; Siliconix, Santa Clara, CA) differential input stage followed by a second stage comprised by an operational amplifier (OPA101; Burr-Brown Corp., Tucson, AZ). Switching between five feedback resistors (500 kΩ, 5 MΩ, 50 MΩ, 500 MΩ, and 10 GΩ) was accomplished using reed relays (Coto, Providence, RI) located in the headstage and configured to minimize their contribution to overall noise. The clamp was designed to have a wideband response (-3dB bandwidth ≥ 50 kHz for all resistors except 10 GΩ) and achieve a frequency response that would be essentially independent of capacitive loads at the input (i.e., the bilayer capacitance) up to ~500 pF. This was accomplished by deliberately increasing the time constant of each of the feedback resistors (except 10 GΩ) by adding a small parallel capacitor. The reduced frequency response was restored by a high frequency "boost" circuit of the type traditionally used in patch voltage clamps employing gigohm range feedback resistors (see, e.g., Rae and Levis, 1984). The utility of this procedure is demonstrated in the Appendix.

Two methods were used to measure the membrane capacitance. In the first, we used the quadrature technique of Neher and Marty (1982). A reference 10 mV peak-to-peak, 1,000 Hz sine-wave, was applied across the membrane and the membrane current converted to voltage by the clamp. This output voltage was passed to a two-channel lock-in amplifier (EG&G 5208; Princeton Applied Research, Princeton, NJ). The time constant of the lock-in output was 10 ms. The in-phase (conductance) and out-of-phase (capacitance) components from the lock-in were digitized and a display of each, generated by modified video date-time generators (Video Timer VTG-33; For-A Corp., West Newton, MA), was superimposed on the video image. In this way, the measured capacitance was synchronized to the observed degree of thinning on a field-by-field (60 Hz) basis. The capacitive component of the lock-in output was also sent to a chart recorder. The phase difference between the reference and clamp signals due to series resistance and stray capacitance was determined with calibrated capacitive loads at the input of the voltage clamp (Neher and Marty, 1982), and was only -0.5 to -0.8°. The signal from the clamp was advanced this amount at the input of the lock-in, minimizing contamination of the capacitive and conductance components by each other. Standard curves relating the output from the lock-in to the input capacitance were generated by using capacitors of known value.

In the second method, the frequency-dependent admittance of the fully thinned membrane was measured with a spectrum analyzer (Dynamic Signal Analyzer 3523A; Hewlett-Packard Co., Palo Alto, CA). The membrane was clamped to a white noise voltage command (Noise

Generator 3722A; Hewlett-Packard Co.). The magnitude and phase shift of each frequency component of the membrane current were computed by the analyzer and stored on disk.

## RESULTS

The basic observation that MM membranes form via a thinning process is illustrated by Fig. 1. Both monolayers have been raised above the hole in *B*, but as determined visually the thinning process had not yet begun. The capacitance (the four left-most digits in the lower left-hand corner; see *A* for schematic and the figure legend for details) remained small. As the hydrocarbon drained out, a front separating the thin from the thick region advanced. Thin and thick regions were distinguished by an unambiguous difference in opalescence. In Fig. 1, the thinned region is advancing bottom to top.<sup>1</sup> In *C-E*, a progressively larger region of thinned bilayer is observed. In *F*, a fully thinned membrane with a surrounding torus is shown. As the membrane thins, a correspondingly larger capacitance is measured as is seen from the progressively larger values of the digital capacitance display. The time course for the increase in membrane capacitance therefore reflects the degree of thinning. Fig. 2 shows a record for the capacitance as a function of time after two solutions have been raised above the hole. The time course for the rise in capacitance is on the order of seconds<sup>2</sup> and has a sigmoidal

<sup>1</sup>Images observed on the monitor are optically inverted. Therefore, the membrane is really thinning top to bottom, not bottom to top as seen in Fig. 1.

<sup>2</sup>The rise times for the capacitance increases varied from on the order of a second to tens of seconds.

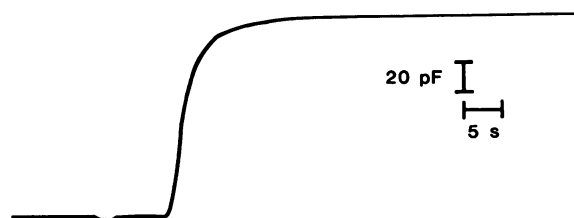


FIGURE 2 Time course for the increase in membrane capacitance. Asolectin monolayers were raised above a 160-μm hole pretreated with squalene.

FIGURE 1 Membranes made by raising monolayers form by a thinning process. *A* is a schematic for the meaning of the digital display. For the display in the lower left-hand corner, the four left-most digits give the measured capacitance in volts (01 . . 55 = 1.55 V = 100 pF). The other eight digits give the time in hours, minutes, seconds, and hundredths of seconds as illustrated. For the digital display in the upper left-hand corner, the four left-most digits give the measured conductance in volts. The conductance of the membrane was small, always well below the resolution of the lock-in, which was set to accommodate the capacitive load. Therefore, the digital display of conductance shows all zeroes, indicating a high resistance membrane. (The slight offset in times seen in the upper and lower digital time display was due to the mechanical difficulty in pushing two buttons at once.) In *B*, both asolectin monolayers have been raised above a squalene-treated hole. The membrane is thick, and the output voltage of the capacitive component from the lock-in amplifier is 0.31 V = 20 pF. In *C-E*, the membrane is seen to thin, initially from the bottom, with concomitant increases in capacitance. In *F*, a fully thinned membrane with a supporting torus (and a microlens at 4 o'clock) is seen. For each panel, the entire portion of thinned membrane was in focus. Distortions in the photograph, such as curvatures of the digits, did not exist on the video monitor from which measurements were taken. Such distortions are seen because the photographs were taken with a macrolens, which does not have a completely flat field.

shape, which is typical for the squalene-treated holes. When the holes were pretreated with Vaseline, the capacitance increase often exhibited a more complex time course, with two or more components evident.<sup>3</sup>

To quantify the specific capacitance, the area of bilayer membrane was evaluated. We focused through the membrane and located the bilayer at the center of the depth of field. As can be seen in Fig. 1 *F*, a visible boundary separated the thinned bilayer from the torus. At the center of the depth of field, small changes in focus caused contrast reversal in the banding pattern surrounding this visible boundary. We always verified that the thinned membrane was optically flat throughout its area (depth of focus 5–10  $\mu\text{m}$ ), thereby ensuring that the membrane was not bulged. This was routinely accomplished by raising the solution on the two sides of the partition to the same level. In control experiments, the membrane was bulged by altering the levels of the aqueous phases. As expected, this manipulation resulted in small increases in capacitance. However, we noted that such bulging also altered the position of the visible boundary within the hole, and the torus changed in size. The major and minor axes of the separating boundary were measured from the video monitor, and the area of the flat bilayer was computed assuming the membrane to be an ellipse. As we could locate each end of an axes to within 1  $\mu\text{m}$ , the maximum error in the measured length of an axes was 2  $\mu\text{m}$ . Therefore, for a 100- $\mu\text{m}$  diam membrane, the maximum error in membrane area should not exceed 4%.

The net capacitance of the bilayer was taken to be the final total value of the measured capacitance minus the background capacitance. The background capacitance, typically 10–15% of the total capacitance, was measured when the first monolayer was raised above the hole, but the second monolayer was just below the hole. We thus assumed that the torus contributed negligible capacitance. In this manner, we determined the specific capacitance of the bilayer when the hole was pretreated with squalene to be  $0.70 \pm 0.10 \mu\text{F}/\text{cm}^2$  mean  $\pm$  SD for asolectin,  $0.79 \mu\text{F}/\text{cm}^2$  for bacterial PE,  $0.65 \pm 0.08 \mu\text{F}/\text{cm}^2$  for TPE, and  $0.94 \pm 0.27 \mu\text{F}/\text{cm}^2$  for DPC. These results are summarized in Table I.

For the above measurements to be reliable, it is necessary that the clamp has sufficient bandwidth and that the frequency characteristics be independent of the capacita-

<sup>3</sup>Petroleum jelly (Vaseline) consists of nonstraight-chain solid and liquid hydrocarbons held within micelles (Schindler, 1961). We contacted Cheesbrough-Ponds, explained how we were using the product, that it had interesting properties, and requested more detailed information on its content. After repeated inquiries, we obtained a letter explaining that the company is not responsible for any harm their product might cause when applied in ways other than for the intended use. A further request for product information resulted in our receiving a one dollar refund, which we used to purchase generic petroleum jelly. It too exhibited a complex time course for thinning.

TABLE I  
SPECIFIC CAPACITANCE,  $C_m$ , OF MEMBRANES FORMED FROM VARIOUS LIPIDS

Phospholipid	$C_m$ (lock-in)	$n$	$d$	$C_m$ (transfer)	$n$	$d$
	$\mu\text{F}/\text{cm}^2$		$nm$	$\mu\text{F}/\text{cm}^2$		$nm$
Asolectin	$0.70 \pm 0.10$	7	2.8	$0.86 \pm 0.13$	5	2.3
BPE	0.79	1	2.5	$0.78 \pm 0.32$	3	2.5
TPE	$0.65 \pm 0.08$	7	3.0	$0.87 \pm 0.34$	4	2.2
DPC	$0.94 \pm 0.27$	6	2.1	$0.78 \pm 0.16$	5	2.5

Values are the mean and SD for  $n$  measurements.

tive load. We determined the frequency characteristics of the clamp by passing white noise through an integrator and sending this integrated noise via a capacitor to the negative input of the headstage. The magnitude of the admittance thus determined (input current/output voltage) was independent of frequency out to 50 kHz ( $-3 \text{ dB attenuation} \geq 50 \text{ kHz}$ ), and in this respect the clamp was close to ideal. When white noise (not integrated) was applied across a solid sheet of Teflon bathed by buffer, the transfer function shown in Fig. 3 *A* was obtained. The magnitude of the transfer function increased linearly with frequency, as theoretically expected for a pure capacitor, although there was a small but noticeable rolloff at higher frequencies. The phase shift was  $45^\circ$  for the Teflon partition at 42 kHz. But the frequency at which the phase shift was  $45^\circ$  varied somewhat with the load capacitance, due to the nonideality of the clamp. The  $45^\circ$  phase shift occurred at 29 kHz for the bilayer whose transfer function is shown in Fig. 3 *B*. For the bilayer, the magnitude increased linearly with frequency, showing that the transfer function was dominated by the capacitance at frequencies above a few hertz. This occurred because the capacitive admittance,  $2\pi f C_m$ , was much larger than the membrane conductance,  $10^{-8} \text{ S}/\text{cm}^2$ . Deviations from linearity due to the voltage clamp frequency response are, however, evident for high frequencies. For practical purposes, the bandwidth of the clamp is adequate and sufficiently insensitive to load capacitance to allow reliable measurements of capacitance to be performed with a lock-in amplifier at 1 kHz.

As the Teflon is electrically in parallel with the membrane, the admittance of the membrane,  $Y_m$ , was obtained by subtracting the admittance when one monolayer was above the hole and the other just below the hole from the total admittance in the presence of a thinned membrane. The specific capacitance of the membrane,  $C_m$ , was calculated from the equation

$$C_m = \frac{Y_m}{2\pi f R_f A},$$

where  $Y_m$  was evaluated in its linear range,  $f$  is the frequency,  $R_f$  is the resistance of the feedback resistor of the head stage, and  $A$  is the area of the membrane. By this method, the specific capacitances for membranes formed

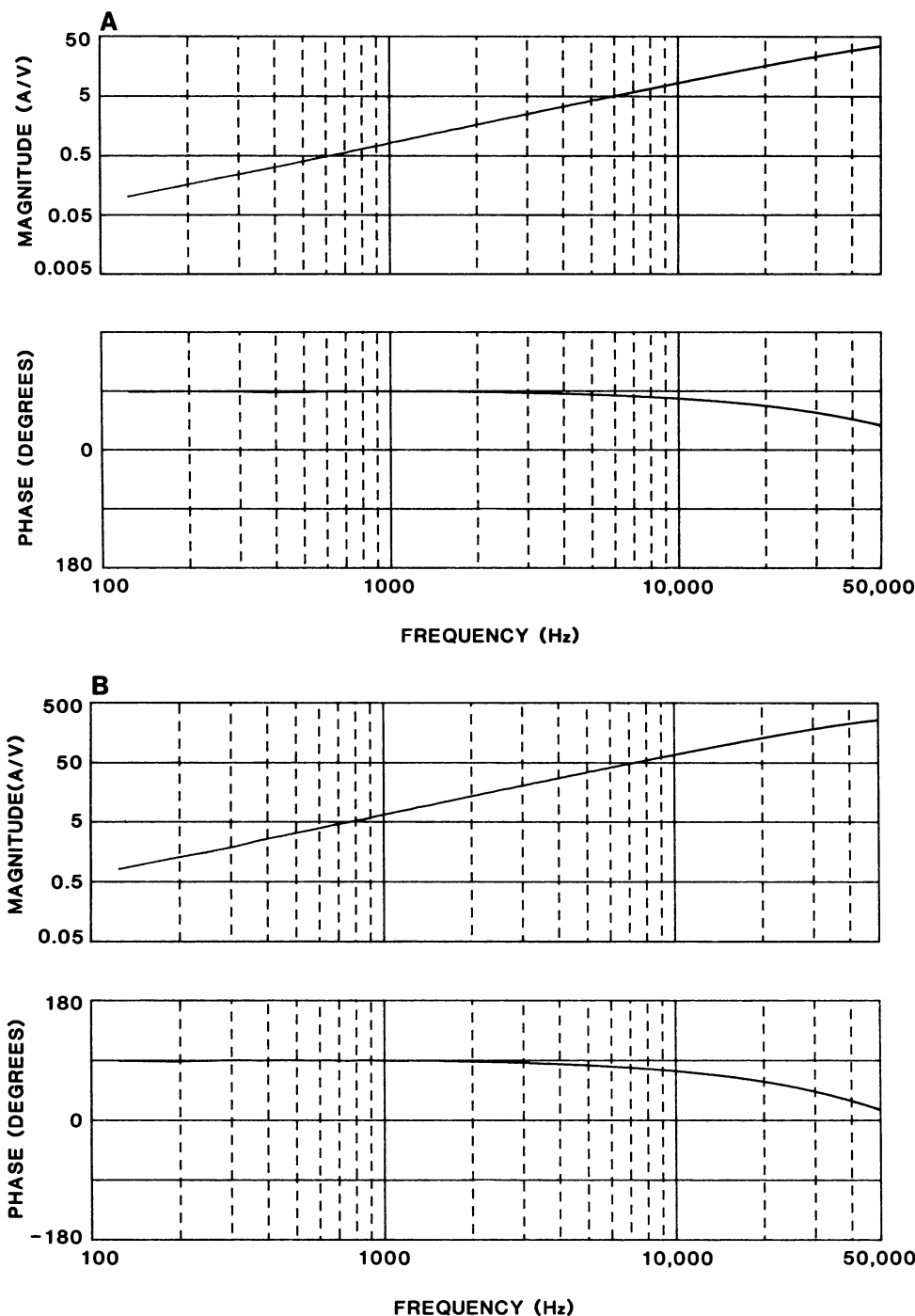


FIGURE 3 Transfer functions. (A) The transfer function of 1-mL Teflon bathed by buffer. (B) Transfer function of an asolectin membrane in a 160- $\mu$ m diam hole pretreated with squalene. The calculated capacitance of the membrane is 149 pF. Note the different scales for the magnitude in A and B.

from various lipid mixtures were obtained and are shown in Table I.

#### DISCUSSION

The formation of MM membranes is customarily described and depicted (Montal and Mueller, 1972; Montal, 1974; White et al., 1976) to be the result of two monolayers directly collapsing onto each other as they are sequentially raised above an aperture. By observing the formation of these membranes with high magnification

microscopy (rather than with dissecting microscopes which are normally employed), it is apparent that contrary to the above view, these membranes form by basically the same thinning procedure that occurs with BLMs. It is a common observation that the growth in capacitance lags, rather than occurs simultaneously with, the raising of both monolayers above the hole. The thinning process naturally explains this observation. When squalene or Vaseline are used as coating solvents, the thinning times are on the order of a few seconds, which is faster than usually occurs with

alkane-based BLMs. The MM membranes contain less solvent as is apparent from their larger capacitances.

The thickness of the hydrocarbon core,  $d$ , was computed from  $C_m = \epsilon_0 \epsilon / d$ , where  $\epsilon_0 = 8.85 \times 10^{-12}$  F/m is the permittivity of free space and  $\epsilon$  is the dielectric constant of the core.  $\epsilon$  has been estimated to range from 2.1 to 2.2 by a variety of independent techniques (White, 1978; Requena and Haydon, 1975*b*; Dilger et al., 1982). We assumed  $\epsilon = 2.2$ . The calculated thicknesses, which correspond to the thickness of the hydrocarbon core, are shown in Table I. The variability in the measured capacitance leads to variabilities in thicknesses. Determining the thickness of the hydrocarbon core is of some practical importance as this thickness is sometimes used to establish detailed models of membrane structure on the molecular level. For instance, recently the depth water penetrates within the headgroup has been estimated by subtracting the thickness of the low dielectric region (determined from capacitance measurements) from the distance between head groups (determined by x-ray diffraction) (Simon and McIntosh, 1986). As extensive capacitance measurements of MM films have assumed the area of the orifice to be that of the membrane, specific capacitance has been underestimated and thicknesses overestimated.<sup>4</sup> A torus was previously inferred to exist in MM films on theoretical grounds (White et al., 1976), and in this study we directly observed such a structure.

The variability in measured capacitance was due to variation between membranes, and not due to the measurements. Lock-in and transfer function measurements were reproducible and agreed with each other to within 4% when fixed capacitors were used. Furthermore, a one-way analysis of variance of the specific membrane capacitances showed that data obtained by the two approaches were identically distributed at an attained level of significance >40%. Variations in measuring capacitance combined with the errors in determining membrane areas are therefore less than the measured variations in specific capacitance. Our observations of specific capacitance are normally distributed for each phospholipid as determined at a 5% level of significance (two-tailed), indicating that with sufficient measurements the mean specific capacitance of a membrane with a given phospholipid composition can be obtained. A complicating factor is, however, that after the initial rapid increase in capacitance due to thinning (Fig. 2), we usually observed a small but steady increase in capacitance (without a concomitant increase in membrane area) over the course of ~1 h. This variable capacitance is symptomatic of lack of thermodynamic equilibrium. That it is difficult to reach equilibrium with diacylphospholipid/

hydrocarbon mixtures is well known (White, 1986). Protocols to reach equilibrium with BLMs prepared from phospholipid/alkane mixtures have been developed (Requena and Haydon, 1975*a*). Procedures to reach equilibrium with MM films have not been as rigorously evaluated. Therefore, those details of structural models of phospholipid bilayers that critically depend on the quantitative values of capacitances obtained from MM films need to be evaluated.

The capacitance of the membrane changed during thinning by about an order of magnitude. Because the series resistance was small (<1 k $\Omega$ ), it did not introduce a significant phase shift (<1 $^\circ$ ), and the capacitive current was simply 90 $^\circ$  out of phase with the input reference voltage. This allowed the capacitance to be measured over a large dynamic range without need to adjust the phase of the lock-in. When capacitance changes are measured in whole-cell patch clamp experiments, the series resistance, due to the pipette, is relatively large (1–5 M $\Omega$ ) and introduces a phase shift that must be adjusted on the lock-in (Neher and Marty, 1982). Small perturbations in capacitance can be reliably measured, but the phase angle of the lock-in must be readjusted when large changes in capacitance occur.

We suggest that Fig. 4 represents the dynamics of membrane formation. In Fig. 4 *A*, both monolayers are still below the hole that has been treated with squalene (we choose this hydrocarbon to discuss a concrete example). The squalene tends to ball up into beads as illustrated. While the first monolayer is being raised, the solution sweeps squalene on top of it as illustrated for the left-hand monolayer of Fig. 4 *A*. Lipid monolayers form at the squalene–water interfaces. After the first solution has been raised above the hole, squalene plugs the hole and a phospholipid monolayer exists at the squalene–water interface as depicted in Fig. 4 *B*. As the second solution is raised above the hole, the sequence just described repeats itself. Immediately after both monolayers have been raised above the hole, squalene is sandwiched between the two monolayers, as shown in Fig. 4 *C*. At this stage, the capacitance is still small (e.g., as in 1 *B*). As the squalene drains out (as in Fig. 1, *C–E*), the sandwich thins until a bilayer forms (Fig. 4 *D*), and the capacitance increases. This picture is in accordance with the common observation that the capacitance continues to grow after the solutions have been raised above the hole. The scheme of Fig. 4 is also consistent with the procedure one uses when forming membranes. One of the solutions is raised above the hole and thereafter is not adjusted. If a membrane does not form, or breaks, the second solution is lowered below the hole and, often, one then blows air around the partition and through the hole, clearing out all the water from the partition on the lowered side. Squalene with a lipid monolayer again plugs the hole, as illustrated in Fig. 4 *B*, rather than an air–water interface forming within the hole because the interfacial tension of an oil–air interface is less

<sup>4</sup>We do note that measurements of specific capacitance of membranes painted from a glycerol monooleate/squalene mixture where the torus was observed (White, 1978; Dilger et al., 1982) gave results consistent with measurements of capacitance of MM membranes formed from the same lipid (Benz et al., 1975; Alvarez and Latorre, 1978).

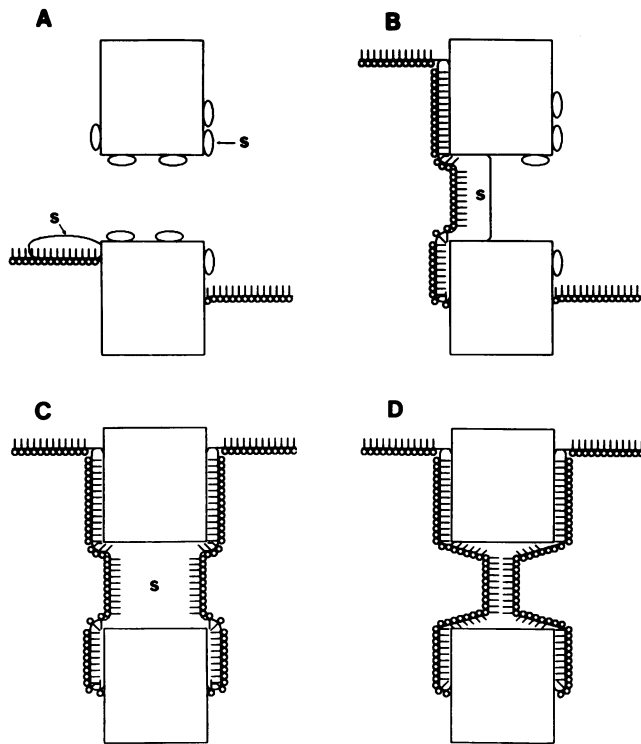


FIGURE 4 Illustration of the formation of membranes made by raising monolayers. (A) The monolayers are still below the hole, but the left-hand monolayer is being raised. The hydrocarbon coating the hole (e.g., squalene), denoted by the letter S, is swept along by the rising monolayer. (B) The left-hand monolayer has been raised above the hole. Squalene plugs the hole, and a phospholipid monolayer exists at the squalene-water interface. (C) Both monolayers have been raised above the hole. A thick membrane consisting of squalene with phospholipid monolayers at each squalene-water interface fills the hole. (D) The membrane has thinned, and a solvent-free bilayer with supporting torus fills the hole. In practice, the thinning process can occur while the second monolayer is being raised above the hole.

than that of a water-air interface. In practice, sufficient squalene is added to ensure that the configurations illustrated by Fig. 4, B and C occur.

In the above scheme for membrane formation, one does not expect, a priori, that the thinned membrane be devoid of solvent. This depends solely on the choice of hydrocarbon that is used to coat the partition. As has been discussed previously (Benz et al., 1975; White et al., 1976; Alvarez and Latorre, 1978), the measured capacitances of MM membranes that use petroleum jelly or squalene as the coating solvent correspond to virtually solvent-free bilayers. This is consistent with the finding that the exclusion of a hydrocarbon from the bilayer region increases as its chain-length increases (Benz et al., 1975; White, 1975), that squalene partitions poorly into phospholipid bilayers (Simon et al., 1977), and with theoretical considerations (Gruen, 1981). Furthermore, it is established that asymmetric membranes can be formed by the method of raising monolayers (Montal, 1973; Hall and Latorre, 1976). This indicates that there is little mixing of

lipid between the two monolayers during the configuration of Fig. 4 C and any such mixing is negligible compared with lipid mixing within a monolayer due to the lateral diffusion.

## APPENDIX

In this Appendix, we elaborate on the use of a capacitor across each feedback resistor to achieve a frequency response that is independent of capacitive load. Consider the circuit shown in Fig. A1. While this figure is somewhat oversimplified, it demonstrates the principles involved. If the open-loop frequency response of the amplifier is approximated by a single pole roll-off, then the transfer function is given by

$$V_o \approx \frac{iR_f}{1 + s(\tau_f + \tau_u) + s^2\tau_u(\tau_L + \tau_f)}, \quad (\text{A1})$$

where  $s$  is the Laplace transform variable ( $s = j\omega$ ),  $\tau_u = 1/(2\pi f_u)$ , and  $f_u$  is the open loop unity gain frequency in hertz,  $\tau_f = R_f C_f$  and  $\tau_L = R_f C_L$ . Note that  $C_L$  is the parallel combination of load capacitance, and the amplifier input capacitance plus strays; it can vary from a minimum of  $\sim 10$  pF (with the input open circuited) to as much as 1,000 pF (with a 300–400- $\mu\text{m}$  diam bilayer).

We illustrate the consequence of Eq. A1 with examples. Consider an amplifier with  $\tau_u = 10^{-8}$  s ( $f_u = 16$  MHz) and a 50-M $\Omega$  feedback resistor. The minimum value of  $C_f$  is  $\sim 0.2$  pF, arising simply from stray capacitance around the resistor. For  $R_f = 50$  M $\Omega$  and  $C_f = 0.2$  pF,  $\tau_f = 10$   $\mu\text{s}$ ; with  $C_L = 10$  pF, the transfer function has two real poles located at 16.8 and 301 kHz. The lower frequency pole is located near  $1/2\pi\tau_f$  as intuitively expected. However, as  $C_L$  increases, the frequency of the first pole increases and that of the second pole decreases until for  $C_L = 50$  pF both poles are located at 31.8 kHz. For all values of  $C_L > 50$  pF, the poles form a complex conjugate pair and therefore the output will "ring" in response to a step change of current. Moreover, as  $C_L$  increases, both the natural frequency and damping factor of the poles decrease, i.e., the response becomes slower and the ringing becomes more severe. Indeed, by the time  $C_L$  has increased to 1,000 pF, the natural frequency has declined to 7.1 kHz and the damping factor is 0.22; the response to a current step will overshoot by 50% and require about half a millisecond to settle to within 1% of its final value. This situation is clearly unacceptable unless the highest frequency of interest is substantially  $< 7$  kHz.

If  $C_f$  is deliberately increased to 2 pF,  $\tau_f$  becomes 100  $\mu\text{s}$ , and it is found that with  $C_L = 10$  pF, the transfer function now has two real poles located at 1.59 kHz ( $\approx 1/2\pi\tau_f$ ) and 2.65 MHz. With  $C_L = 100$  pF, the pole frequencies become 1.60 and 155 kHz, and with  $C_L = 1,000$  pF, the pole frequencies become 1.68 and 30 kHz. Thus, although the first pole has moved to a lower frequency in comparison with the result for  $C_f = 0.2$  pF,

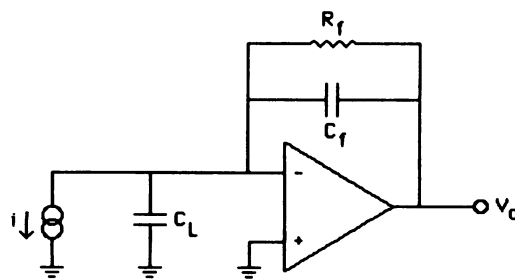


FIGURE A1 Schematic showing a capacitor across a feedback resistor of the voltage-clamp headstage. For simplicity the membrane is represented by a current source in parallel with a capacitance load.

its location is more stable with changes in  $C_L$ .<sup>5</sup> The performance achieved with  $C_f = 2$  pF is thus considerably improved, but the desired independence of frequency response has not been fully achieved. The problem is that with  $C_L = 1,000$  pF, the secondary pole (located at 30 kHz) will restrict the final boosted bandwidth, and the small (5%) increase in the first pole frequency will mean that the setting of the boost circuit established in the absence of a bilayer membrane will no longer be appropriate, resulting in a step response with a small overshoot (~5%), decaying with a 100- $\mu$ s time constant for  $C_L = 1,000$  pF.

Therefore, consider the consequence of increasing  $C_f$  to 20 pF ( $\tau_f = 1$  ms). With  $C_L = 10$  pF, the transfer function has two real poles at 159.16 Hz and 10.6 MHz. With  $C_L = 100$  pF, the pole frequencies become 159.17 Hz and 2.65 MHz, and with  $C_L = 1,000$  pF, they become 159.24 Hz and 312 kHz. In this situation, the frequency of the first pole varies by only ~0.05% as  $C_L$  changes from 10 to 1,000 pF. The frequency of the second pole declines dramatically as  $C_L$  increases, but even with a 1,000 pF load, it remains at a sufficiently high frequency to have no significant effect in the frequency range of interest. A 20-MHz boost amplifier could theoretically increase the bandwidth from 159 Hz to ~56 kHz; in actual practice ~35 kHz can readily be achieved.

The consequences arising from capacitive loading of the input of the current to voltage converter ("headstage") that was illustrated in the above examples can be understood more generally by referring to eq. A1. For any given value of  $C_f$ , the value of the coefficient of  $s$  (call this coefficient  $A$ ) is fixed; however, as  $C_L$  increases, the coefficient of  $s^2$  (call this coefficient  $B^2$ ) increases. To avoid a complex conjugate pair of poles (with a "ringing" step response), it is required that  $A \geq 2B$ . Moreover, if both poles are real and if the lower frequency pole is to remain at a more or less constant location, it is necessary that  $A \gg B$  for all anticipated values of  $B$  (i.e., of  $C_L$ ). In the above example, it was assumed that  $\tau_u$  was  $10^{-8}$  s ( $f_u = 16$  MHz). Examination of Eq. A1 shows that the condition  $A \gg B$  can be achieved with smaller values of  $\tau_f$  if  $\tau_u$  is decreased ( $f_u$  is increased). Gain-bandwidth products substantially larger than 16 MHz can readily be achieved, although it is difficult for a unity gain stable amplifier to do much better.<sup>6</sup> It should also be noted that  $B$  varies at  $\tau_u^{1/2}$ . Thus, although it is desirable to use the fastest possible amplifier (because of this square root relation), decreasing the value of  $\tau_u$  within practical limits cannot completely solve the problem. Our approach simply increases the value of  $A$  (i.e., of  $\tau_f$ ) to a value that is sufficient to achieve  $A \gg B$  for all values of  $C_L$  that are expected. In our particular implementation, we sometimes used values of  $C_f$  that were smaller than the above considerations would indicate. This was done as a compromise between maintaining a high boosted bandwidth and adequate independence of capacitive loads.

It should be noted that for frequency domain measurements of the type considered in this paper, it is quite possible to calibrate the frequency response for any constant value of  $C_L$ . However, we did not do this because the bilayer capacitance varied during the thinning process. Moreover, such calibration would be of little help for time domain measurements from various sized bilayers.

We implemented switching between feedback resistors with reed

<sup>5</sup>The frequency response of the amplifier, reduced by  $C_f$ , can be increased. A single stage high frequency "boost" circuit employing an amplifier with a unity gain frequency denoted by  $f_{ub}$  can theoretically increase the bandwidth from the "unboosted" headstage output (unboosted bandwidth denoted by  $f_o$ ) to  $(f_o f_{ub})^{1/2}$  (see Levis, 1981; Rae and Levis, 1984). Thus, for  $f_o = 1.6$  kHz, a boost amplifier with  $f_{ub} = 20$  MHz could theoretically produce a boosted bandwidth (natural frequency) of ~180 kHz. Due to higher frequency poles not considered in this analysis, actual performance is somewhat worse, leading to a final bandwidth of ~100 kHz.

<sup>6</sup>Unity gain stability is not necessary in this situation, but to analyze the results with such an amplifier, it is necessary to at least consider the secondary pole in the open loop frequency response. The location of this pole is usually determined by the JFET input stage.

relays. The use of relays causes a small but noticeable increase in the high frequency noise for the highest valued feedback resistors when the input is open circuited; presumably this is due to the lossy dielectric of the plastic in which these devices are embedded. This noise component is not observed with the smaller feedback resistors because it is masked by their higher thermal noise. Furthermore, with any of the feedback resistors, this extra noise is negligible in an actual experimental situation: when currents are measured from lipid bilayer membranes (capacitance > 50 pF), high frequency noise is dominated by the thermal voltage noise of the electrodes plus the convergence resistance to the membrane plus input voltage noise of the headstage amplifier in conjunction with the bilayer capacitance. If measurements were to be obtained from very low capacitance preparations, somewhat lower noise would be achieved using a field-effect transistor switching arrangement.

We thank Messrs. Verlin Giuffre and George Hack for construction of the voltage clamp.

This work was supported by National Institutes of Health grants GM27367 and NS21111.

Received for publication 31 August 1987 and in final form 16 November 1987.

## REFERENCES

- Alvarez, O., and R. Latorre. 1978. Voltage-dependent capacitance in lipid bilayers made from monolayers. *Biophys. J.* 21:1-17.
- Benz, R., O. Frölich, P. Lauger, and M. Montal. 1975. Electrical capacity of black lipid films and of lipid bilayers made from monolayers. *Biochim. Biophys. Acta.* 394:323-334.
- Dilger, J. P., L. R. Fisher, and D. A. Haydon. 1982. A critical comparison of electrical and optical methods for bilayer thickness determination. *Chem. Phys. Lipids.* 30:159-176.
- Gruen, D. W. R. 1981. A mean-field model of the alkane-saturated lipid bilayer above its phase transition. I. Development of the model. *Biophys. J.* 33:149-166.
- Hall, J. E., and R. Latorre. 1976. Nonactin-K<sup>+</sup> complex as a probe for membrane asymmetry. *Biophys. J.* 16:99-103.
- Hanai, T., D. A. Haydon, and J. Taylor. 1965. An investigation by electrical methods of lecithin-in-hydrocarbon films in aqueous solutions. *Proc. R. Soc. Lond. A. Sci.* 281:377-391.
- Kagawa, Y., and E. Racker. 1971. Partial resolution of the enzymes catalyzing oxidative phosphorylation. *J. Biol. Chem.* 246:5477-5487.
- Levis, R. A. 1981. Patch and axial wire voltage clamp techniques and impedance measurements from cardiac Purkinje fiber. Ph.D Thesis, University of California, Los Angeles.
- Montal, M. 1973. Asymmetric lipid bilayers: response to multivalent ion. *Biochim. Biophys. Acta.* 298:750-754.
- Montal, M. 1974. Formation of bimolecular membranes from lipid monolayers. *Methods Enzymol.* 32:545-554.
- Montal, M., and P. Mueller. 1972. Formation of biomolecular membranes from lipid monolayers and a study of their electrical properties. *Proc. Natl. Acad. Sci. USA.* 69:3561-3566.
- Mueller, P., D. O. Rudin, H. T. Tien, and W. C. Wescott. 1963. Methods for the formation of single bimolecular lipid membranes in aqueous solution. *J. Phys. Chem.* 67:534-535.
- Neher, E., and A. Marty. 1982. Discrete changes of cell membrane capacitance observed under conditions of enhanced secretion in bovine adrenal chromaffin cells. *Proc. Natl. Acad. Sci. USA.* 79:6712-6716.
- Niles, W. D., and F. S. Cohen. 1987. Video fluorescence microscopy studies of phospholipid vesicle fusion with a planar phospholipid membrane. Nature of membrane-membrane interactions and detection of contents release. *J. Gen. Physiol.* 90:703-735.
- Rae, J. L., and R. A. Levis. 1984. Patch voltage clamp of lens epithelial cells: theory and practice. *Mol. Physiol.* 6:115-162.
- Requena, J., and D. A. Haydon. 1975a. The Lippmann equation and the

- characterization of black lipid films. *J. Colloid Interface Sci.* 51:315–327.
- Requena, J., and D. A. Haydon. 1975b. Van der Waals forces in oil-water systems from the study of thin lipid films. II. The dependence of the van der Waals free energy of thinning of film composition and structure. *Proc. R. Soc. Lond. A. Sci.* 347:161–177.
- Reyes, J., and R. Latorre. 1979. Effect of the anesthetics benzyl alcohol and chloroform on bilayers made from monolayers. *Biophys. J.* 28:259–280.
- Schindler, H. 1961. Petrolatum for drugs and cosmetics. *Drug Cosmet. Ind.* 89:36.
- Simon, S. A., T. J. Lis, R. C. MacDonald, and J. W. Kauffman. 1977. The noneffect of a large linear hydrocarbon, squalene, on the phosphatidylcholine packing structure. *Biophys. J.* 19:83–90.
- Simon, S. A., and T. J. McIntosh. 1986. Depth of water penetration into lipid bilayers. *Methods Enzymol.* 127:511–521.
- Takagi, M., K. Azuma, and U. Kishimoto. 1965. A new method for the formation of bilayer membranes in aqueous solution. *Annu. Rep. Biol. Works Fac. Sci. Osaka Univ.* 13:107–110.
- White, S. H. 1972. Analysis of the torus surrounding planar bilayer membranes. *Biophys. J.* 12:432–445.
- White, S. H. 1975. Phase transitions in planar bilayer membranes. *Biophys. J.* 15:95–117.
- White, S. H. 1978. Formation of “solvent-free” black lipid bilayer membranes from glycerol monooleate dispersed in squalene. *Biophys. J.* 23:337–347.
- White, S. H. 1986. The physical nature of planar bilayer membranes. *In* Ion Channel Reconstitution. C. Miller, editor. Plenum Publishing Corp., New York. 3–35.
- White, S. H., D. C. Petersen, S. Simon, and M. Yafuso. 1976. Formation of planar bilayer membranes from lipid monolayers: a critique. *Biophys. J.* 16:481–489.